AMERICAN ACADEMY™
OF OPHTHALMOLOGY

Characterization of Chorioretinopathy Associated with Mitochondrial Trifunctional Protein Disorders

Long-Term Follow-up of 21 Cases

Erin A. Boese, MD,[1] Nieraj Jain, MD,[2] Yali Jia, PhD,[1] Catie L. Schlechter, MS, CGC,[1] Cary O. Harding, MD,[3] Simon S. Gao, PhD,[1] Rachel C. Patel, BA,[1] David Huang, MD, PhD,[1] Richard G. Weleber, MD,[1] Melanie B. Gillingham, PhD,[3] Mark E. Pennesi, MD, PhD[1]

Purpose: To assess long-term effects of genotype on chorioretinopathy severity in patients with mitochondrial trifunctional protein (MTP) disorders.

Design: Retrospective case series.

Participants: Consecutive patients with MTP disorders evaluated at a single center from 1994 through 2015, including 18 patients with long-chain 3-hydroxyacyl-CoA dehydrogenase deficiency (LCHADD) and 3 patients with trifunctional protein deficiency (TFPD).

Methods: Local records from all visits were reviewed. Every participant underwent a complete ophthalmic examination and was evaluated by a metabolic physician and dietitian. Nine patients underwent ancillary funduscopic imaging including optical coherence tomography (OCT) and OCT angiography.

Main Outcome Measures: The primary outcome measure was best-corrected visual acuity at the final visit. Secondary outcome measures included spherical equivalent refraction, visual fields, electroretinography B-wave amplitudes, and qualitative imaging findings.

Results: Participants were followed up for a median of 5.6 years (range 0.3–20.2 years). The median age of LCHADD participants at initial and final visits was 2.3 and 11.9 years, whereas that for TFPD participants at initial and final visits was 4.7 and 15.5 years, respectively. Four long-term survivors older than 16 years were included (3 with LCHADD and 1 with TFPD). The LCHADD participants demonstrated a steady decline in visual acuity from an average of 0.23 logarithm of the minimum angle of resolution (logMAR; Snellen equivalent, 20/34) at baseline to 0.42 logMAR (Snellen equivalent, 20/53) at the final visit, whereas TFPD patients maintained excellent acuity throughout follow-up. Participants with LCHADD, but not TFPD, showed an increasing myopia with a mean decrease in spherical equivalent refraction of 0.24 diopters per year. Visual fields showed sensitivity losses centrally associated with defects on OCT. Multimodal imaging demonstrated progressive atrophy of the outer retina in LCHADD, often preceded by the formation of outer retinal tubulations and choriocapillaris dropout. Electroretinography findings support the more severe clinical profile of LCHADD patients compared with TFPD patients; the function of both rods and cones are attenuated diffusely in LCHADD patients, but are within normal limits for TFPD patients.

Conclusions: Despite improved survival with early diagnosis, medical management, and dietary treatment, participants with the LCHADD subtype of MTP disorder continue to demonstrate visually disabling chorioretinopathy. Multimodal imaging is most consistent with choriocapillaris loss exceeding photoreceptor loss. *Ophthalmology 2016;■:1–13 © 2016 by the American Academy of Ophthalmology.*

Supplemental material is available at www.aaojournal.org.

Mitochondrial trifunctional protein (MTP) disorders are rare, recessively inherited conditions of impaired fatty acid metabolism. Affected patients typically seek treatment at an early age with episodes of hypoketotic hypoglycemia, cardiomyopathy, rhabdomyolysis, hepatomegaly, and sudden death.[1–5] Early recognition and initiation of treatment including dietary modifications have improved survival considerably, and many patients are now living into adulthood.[6,7] Despite these advances, most patients experience progressive and advanced visual disability.[8–12]

Mitochondrial trifunctional protein disorders result from mutations within the trifunctional protein (TFP), a protein complex that catalyzes 3 specific enzymatic activities in long-chain fatty acid metabolism: 2-3 enoyl

http://dx.doi.org/10.1016/j.ophtha.2016.06.048
ISSN 0161-6420/16

CoA hydrase, long-chain 3-hydroxyacyl-CoA dehydrogenase (LCHAD), and 3-ketoacyl-CoA thiolase. Long-chain 3-hydroxyacyl-CoA dehydrogenase deficiency (LCHADD; Online Mendelian Inheritance in Man identifier, 609016) is defined by the presence of the common mutation c.1528G→C in at least 1 allele of the *HADHA* gene, which yields a normal protein expression of the enzyme complex and a predominant deficiency of LCHAD activity with relative sparing of the other 2 enzymatic activities. Other mutations within the *HADHA* or *HADHB* genes are associated with decreased protein expression and more uniform deficiency of all 3 enzymatic activities, yielding so-called multifunctional TFP deficiency (TFPD; Online Mendelian Inheritance in Man identifier, 609015). Although resulting from a similar disruption in fatty acid metabolism, TFPD has several distinct differences, including the absence of liver pathologic features and a milder ocular phenotype.[1,2,13]

We previously reported the 5-year results of a prospective study correlating medical treatment and dietary patterns with chorioretinopathy progression in MTP disorders that demonstrated relative retention of retinal function among patients with improved dietary management and lower hydroxyl acylcarnitines.[6] Participants from this initial study, affected by either LCHADD or TFPD, are now among the longest known survivors with the disease. Herein we present long-term findings in 21 participants with up to 20 years of follow-up, exploring the effect of genotype on chorioretinopathy severity. We provide an in vivo structural assessment of the affected retina with multimethod imaging, including optical coherence tomography (OCT), OCT angiography, and fundus autofluorescence (FAF). Using serial electroretinography, we also demonstrate corresponding functional changes with time.

Methods

This was a retrospective case series of all patients seen at the Casey Eye Institute, Oregon Health & Science University (OHSU), between September 20, 1994, and August 18, 2015, with a diagnosis of either LCHADD or TFPD. All participants were followed up clinically or participated in various research protocols in the Department of Molecular and Medical Genetics of OHSU, as detailed previously,[6,7] and 13 of these participants were reported previously in a prospective open-label study evaluating the effect of diet treatment on chorioretinopathy progression.[6] Diagnosis of LCHADD or TFPD was based on the presence of at least 2 of 3 of the following: clinical findings, disease-specific acylcarnitine profiles, or enzymatic assays in cultured skin fibroblasts. All participants underwent molecular testing, which identified 2 deleterious mutations in the *HADHA* or *HADHB* genes in 18 of the 21 cases.

Approval from the OHSU Institutional Review Board for the study protocol and consent were obtained, and the study followed the tenets set forth by the Declaration of Helsinki. Each participant's legal guardian provided informed consent for obtaining outside records, and participants older than 7 years gave assent to participate.

Medical Clinical Evaluation

Participants were evaluated by a biochemical geneticist (C.O.H.) at Doernbecher Children's Hospital or at the Clinical and Translational Research Center of OHSU as part of routine clinical care or a clinical research study, respectively. Patients were asked to maintain a diet low in long-chain fatty acids and were supplemented with medium-chain triglycerides to minimize oxidation, as previously described by Gillingham.[7] Medical history and complete physical examination including neurologic evaluation were completed. Participants in a research study were asked to complete a 3-day diet record and to return the completed record to the investigators (M.B.G.) for analysis. Blood samples were collected after an overnight fast and were analyzed for plasma acylcarnitines by electrospray tandem mass spectrometry at the Biochemical Genetics Laboratory, Mayo Clinic.[14] Dietary intake was assessed by 24-hour dietary recall for patients evaluated clinically by the metabolic dietitian. Nonfasting blood samples were sent for plasma acylcarnitine analysis as described previously.

Ophthalmic Clinical Evaluation

Participants initially underwent a complete ophthalmic examination with cycloplegic refraction and full-field electroretinography (ffERG). Best-corrected visual acuity (BCVA) was measured with Snellen testing and was converted to logarithm of the minimum angle of resolution (logMAR) units. Nine participants underwent additional imaging, including spectral-domain OCT (Spectralis; Heidelberg Engineering, Germany), OCT angiography (Avanti RTVue XR; OptoVue, Inc., Freemont, CA), and wide-field FAF imaging (200Tx; Optos PLC, Freemont, CA) at the discretion of the treating ophthalmologist, often based on the availability of these tests and the patient's ability to cooperate. Severities of chorioretinopathy for and last documented visits were assessed by a retina specialist (N.J.) based on the previously described chorioretinopathy staging system.[12] Fundus images and clinical data were used to stage the chorioretinopathy. For visual acuity and refractive error analysis, our records were supplemented with outside ophthalmology records. Visual fields, including manual and automated kinetic perimetry (Octopus 101 or Octopus 900; Haag-Streit, Koeniz, Switzerland) were obtained from participants old enough to participate. Static visual fields were performed using the same perimeter, a radially designed, centrally condensed grid containing 164 test location[15]; the GATEi strategy[16,17]; and a 200-ms stimulus of size V on a white background of 10 cd/m^2. The reliability factor for the static perimetry was calculated as the sum of positive and negative catch trials divided by the total number of catch trials presented (designated as a percentage). The sensitivity values were imported into a custom software application (United States patent no. 8,657,446, Visual Field Modeling and Analysis, or VFMA, Office of Business and Technology of OHSU) to model the hill of vision. The volumetric indices (in decibel-steradian or dB-sr) of differential luminance sensitivity—V_{tot}, V_{30°, and V_{periph} ($V_{tot}-V_{30^\circ}$)—and defect space—D_{tot}, D_{30°, and D_{periph} ($D_{tot}-V_{30^\circ}$)—were measured from the model as described previously.[15]

En face OCT images of the outer retina and retinal pigment epithelium (RPE) were derived from the mean reflectance of slabs 25 to 45 μm above Bruch's membrane (BM) and 25 μm above BM to BM, respectively. The OCT angiography images were derived

using the split-spectrum amplitude-decorrelation angiography algorithm.[18,19] The en face OCT angiography of the choroid was the maximum flow projection below BM.

Participants underwent ffERG testing (the custom electroretinography unit at Casey Eye Institute, Portland, OR) following the standard of the International Society for Clinical Electrophysiology of Vision.[6,20] A previously described locally developed normative database stratified for age and using the identical machine and testing parameters was used in electroretinography analysis.[6] Most participants were sedated for electroretinography testing until 8 years of age and completed unsedated electroretinography testing at 9 years of age and older.

The primary end point was visual acuity (logMAR) at the final visit. Secondary end points included spherical equivalent refraction, ffERG B-wave amplitudes, ffERG B-wave implicit times, and qualitative imaging findings.

Statistical Methods

Baseline sample characteristics were summarized with means and standard deviations for continuous variables and frequencies and percentages for categorical variables. Snellen best-corrected visual acuities were converted to logMAR values for analysis. Visual acuities of counting fingers first were converted to Snellen acuities based on the assumption that fingers are approximately the size of a 200 letter.[21] Some patients were too young to perform Snellen acuity testing; those visits were not included within the analysis. In all instances, these were measured as central, steady, and maintained and did not differ among participants. For analysis of visual acuity over time, only participants with 2 or more recorded Snellen acuities were included.

Correlation between age and visual acuity (logMAR) for participants with LCHADD and participants with TFPD were calculated using a Pearson correlation for data sets that were normally distributed and Spearman correlation for data sets that were non-normally distributed. The linear fit of the visual acuity versus age was compared between participants with LCHADD and participants with TFPD to determine if the slope or intercept of the line was significantly different between groups. For electroretinography results, right eye and left eye values were averaged and all data points were expressed as an absolute value compared with age and testing conditions (sedated vs. unsedated) and expressed as a *z*-score (value−mean/standard deviation) for that age and testing condition. For all participants with 4 or more electroretinography measurements, we compared the change in *z*-scores over time between groups with a repeated-measures analysis of variance. Prism software version 6.0 (Graphpad, Inc., La Jolla, CA) was used for all analyses, and $P < 0.05$ was considered statistically significant.

Results

Twenty-one participants were followed up for a median of 5.6 years (7.0 years for LCHADD [range, 0.3−20.2 years]; 5.3 years for TFPD [range, 5.2−14.7 years]; Table 1). Median age for LCHADD participants at the initial and final visits was 2.3 years (range, 0.4−17.7 years) and 11.9 years (range, 3.3−24.2 years), and median age for TFPD participants at the initial and final visits was 4.7 years (range, 1.0−10.3 years) and 15.5 years (6.3−19.4 years), respectively. Nine of the 16 LCHADD patients and 2 of 3 TFPD patients were older than 12 years at the final visit. All LCHADD patients were diagnosed within the first 9 months of life (range, birth−9 months), and all TFPD patients were diagnosed by early childhood (range, birth−3 years). Of note, many patients did not undergo ophthalmic examination immediately on diagnosis. During the course of the study, 2 LCHADD participants and 1 TFPD participant died of cardiac complications.

Patient Characteristics

Eighteen of the 21 patients were diagnosed with LCHADD, characterized by the presence of the common mutation (c.1528G→C) in at least 1 allele of the *HADHA* gene. Of these, 9 (50%) were homozygous and 6 (33%) were characterized as compound heterozygotes, containing a variety of known pathogenic mutations as well as novel mutations predicted to be pathogenic. A second mutation was not isolated in 3 participants (16.7%; Table 1). Of the 3 participants with a clinical diagnosis of TFPD, each had the c.901G→A mutation within the *HADHB* gene, although the second mutation was not identified in any patient (Table 1). Two of the 3 participants were siblings and presumably had the same causative mutations.

Participants presented symptomatically with hypoketotic hypoglycemia or rhabdomyolysis or were identified presymptomatically because of the diagnosis of an older sibling (Table 1). All participants, their guardians, or both were counseled to avoid fasting, to follow a low long-chain fat diet, and to consume medium-chain triglyceride supplements. Some participants were prescribed oral carnitine supplements. All participants had at least 1 hospital admission for rhabdomyolysis consistent with metabolic decompensation of LCHAD and TFP deficiencies. Participants consumed approximately 10% to 17% of total energy from long-chain fat and 10% to 20% of energy from medium-chain triglyceride supplements based on available diet recall analysis (Table S1, available at www.aaojournal.org).[6,7] A sum of all the plasma long-chain hydroxyl-acylcarnitine species was calculated. Low metabolite concentrations of less than 1.5 μmol/l were observed in 11 participants, including all 3 participants with TFPD. High metabolite concentrations of more than 1.5 μmol/l were observed in 5 participants with LCHADD.

Visual Acuity

Visual acuity progression was assessed using the mean visual acuity between the 2 eyes at each visit. In participants with LCHADD, mean baseline and final BCVA was 0.23±0.26 logMAR and 0.42±0.31 logMAR (Snellen equivalent, 20/34 and 20/53), respectively. The correlation between age and decrease in visual acuity was significant for participants with LCHADD, but not for participants with TFPD (LCHADD: Spearman $r = 0.88$; $P < 0.001$; TFPD: $r = -0.5$; $P = 0.79$). Taking all BCVA values together, grouped by age, there was a linear decline with slope of approximately 0.034 logMAR units per year among patients with LCHADD ($R^2 = 0.66$) not observed among patients with TFPD (Fig 1A). There was also a notable disparity between the eyes of LCHADD participants. The overwhelming majority (16 of 18 LCHADD patients) retained a final visual acuity of 0.3 logMAR (Snellen equivalent, 20/40) or better in 1 eye, despite a decline with advancing age in the other (Fig 1B; Pearson $r = 0.85$; $P < 0.0001$). The other 2 patients had very advanced disease; on the

Table 1. Baseline Demographics and Clinical Characteristics

Patient Identification	Gender	Age at Diagnosis (yrs)	Age at Eye Visit (yrs)		Follow-up (yrs)	Clinical Presentation	Variant 1	Variant 2	Residual Enzyme Activity (nmol/min/mg of Protein)		History of >1 Episode of Rhabdomyolysis
			First Visit	*Last Visit*					*Long-Chain 3-Hydroxyacyl-CoA Dehydrogenase*	*Ketothiolase*	
LCHADD											
LC01	M	3 mos	4.4	12.5	8.1	Hypoketotic hypoglycemia	G1528C	G1528C	11.8	38.6	Y
LC02	F	9 mos	1.0	15.8	14.8	Hypoketotic hypoglycemia	G1528C	c.274−278del			Y
LC03	F	DOL 3	0.8	5.8	5.0	Hypoketotic hypoglycemia	G1528C	G1528C			Y
LC04	F	DOL 1	4.7	14.3	9.7	Hypoketotic hypoglycemia	G1528C	c.274−278del	10.2	10.7	Y
LC05	M	6 mos	9.5	15.8	6.3	Hypoketotic hypoglycemia	G1528C	Not detected*			Y
LC06	M	4 mos	1.0	7.6	6.6	Hypoketotic hypoglycemia	G1528C	G1528C			Y
LC07	F	Birth, diagnosed sibling	2.5	6.4	3.9	None	G1528C	G1528C			Y
LC08	F	4 mos	2.1	12.7	10.6	Hypoketotic hypoglycemia	G1528C	G1528C	10.7	21.0	Y
LC09	M	5 mos	11.1	16.7	5.6	Hypoketotic hypoglycemia	G1528C	c.1678C→T			Y
LC10	F	3 mos	17.7	18.0	0.3	Hypoketotic hypoglycemia, cardiorespiratory arrest	G1528C	G1528C			Y
LC11	F	5 mos	0.8	3.3	2.4	Hypoketotic hypoglycemia	G1528C	T1678C			Lost to follow-up
LC12	F	NBS	1.4	5.3	3.8	Hypoglycemia	G1528C	Not detected*			Y
LC13	M	6 mos	5.6	9.8	4.2	Hypoketotic hypoglycemia	G1528C	G1528C			Y
LC14	F	6 mos	4.0	24.2	20.2	Hypoketotic hypoglycemia, cardiorespiratory arrest	G1528C	c.479−482T AGC→AATA			Y
LC15	M	Birth, diagnosed sibling	0.4	11.3	10.9	None	G1528C	c.274−278del			Y
LC25	F	NBS	11.8	14.2	2.4	None	G1528C	G1528C			Y
LC27	M	Birth, family history	1.6	9.2	7.6	None	G1528C	G1528C			Y
LC31	M	NBS	1.4	5.4	4.0	None	G1528C	Splice-site mutation (A+3G after exon 3)			N
TFPD											
LC16	F	3 yrs	10.3	15.5	5.2	Rhabdomyolysis	c.901G→A β-subunit	Not detected*			Y
LC17	F	Diagnosed sibling	4.7	19.4	14.7	None	c.901G→A β-subunit	Not detected*	12.4	0.4	Y
LC18	M	DOL 2	1.0	6.3	5.3	Hypoketotic hypoglycemia	c.901G→A β-subunit	Not detected*			Y

DOL = day of life; F = female; LCHADD = long-chain 3-hydroxyacyl-CoA dehydrogenase deficiency; m = male; NBS = newborn screening; TFPD = trifunctional protein deficiency.
*No second mutation identified.

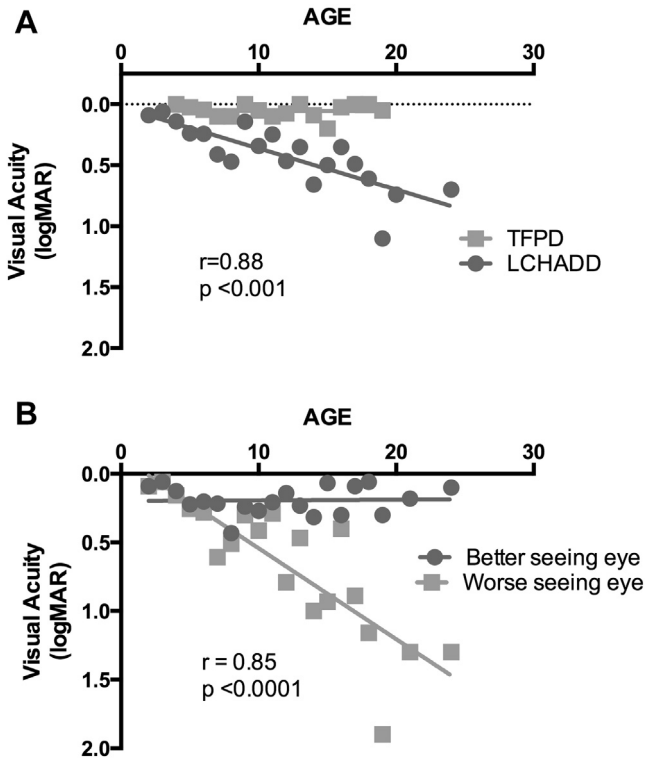

Figure 1. Visual acuity declines in long-chain 3-hydroxyacyl-CoA dehydrogenase deficiency (LCHADD) eyes, but not in trifunctional protein deficiency (TFPD) eyes. **A**, Participants with LCHADD (circles) had a progressive decline in best-corrected visual acuity with increasing age when all visits of all patients were averaged for each age rounded to nearest year, averaging 0.03 logarithm of the minimum angle of resolution (logMAR) acuity loss per year. The data were nonnormally distributed. Spearman correlation between logMAR visual acuity and age was significant ($r = 0.88$; $P < 0.001$). The TFPD patients (squares) maintained excellent visual acuity throughout the study. There was no significant correlation between logMAR visual acuity and age among participants with TFPD. **B**, Best-corrected visual acuity plotted individually for the better-seeing eye (circles) and worse-seeing eye (squares) in LCHADD patients. There was a significant correlation between logMAR visual acuity and age for the worse-seeing eye among participants with LCHADD (Pearson $r = 0.85$; $P < 0.0001$).

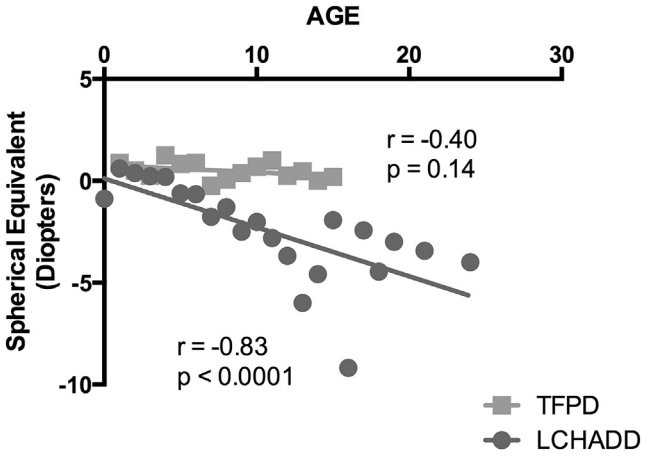

Figure 2. Long-chain 3-hydroxyacyl-CoA dehydrogenase deficiency (LCHADD) patients had progressive myopia. Participants with LCHADD had a significant mean decrease in spherical equivalent with increasing age, averaging 0.24-diopter (D) increase in myopia per year when visits of all patients were averaged for age rounded to nearest year. Conversely, participants with trifunctional protein deficiency (TFPD) had minimal progression of myopia, with spherical equivalent decreasing by 0.03 D per year. The data were nonnormally distributed. Spearman correlation of diopters and age was significant for participants with LCHADD ($r = -0.83$; $P < 0.0001$), but was not correlated significantly for participants with TFPD ($P = 0.14$).

final visit, patient LC02 had visual acuities of 0.8 logMAR and 0.7 logMAR, and patient LC13 had visual acuities of 1.0 logMAR and 0.7 logMAR at ages 15.8 and 9.8 years, respectively. Participants with TFPD all had excellent and stable visual acuity, with mean final visual acuity of 0.02±0.03 logMAR (Snellen equivalent, 20/21; Fig 1A).

Many participants were too young for most of the study to perform visual field testing reliably. Six LCHADD participants and 1 TFPD participant underwent at least 1 visual field test during the course of the study, and a total of 3 LCHADD participants underwent more than 1 visual field test. Patient LC14 underwent a series of visual fields performed over 9.5 years (Figs S1–S3, available at www.aaojournal.org) that demonstrated a progression consistent with prior studies.[11] On kinetic perimetry, this patient had small bilateral paracentral scotomata in each eye on initial testing early in the disease, and with time, these paracentral defects enlarged and deepened (Fig S1, available at www.aaojournal.org). Static testing at 24.2 years of age disclosed a profoundly decreased foveal sensitivity of 14.5 dB (normal, 37.4 dB) and a small ring scotoma within 10° of fixation in the right eye (Fig S2, available at www.aaojournal.org). For the left eye, the sensitivity at foveal fixation was 29.2 dB and was located on the temporal size of a small, irregularly shaped 23.9°^{2} region of sensitivity just nasal to fixation that peaked at 32.4 dB. When viewed in defect space, this small region of preserved field remained throughout its extent within 7.6 dB of normal expected sensitivity (Fig S3, available at www.aaojournal.org).

Refractive Error

Participants with LCHADD had progressive myopia with a mean decline in spherical equivalent of −0.24 diopters (D) per year after a linear trajectory (Spearman correlation between D (diopters) and age, $r = -0.82$; $P < 0.001$; Fig 2). Unlike typical myopic progression that stabilizes by teenage years, patients with LCHADD had a steady myopic decline that continued into early adulthood. Many patients demonstrated high myopia by their teenage years. In contrast to BCVA, there was minimal disparity in refractive error between the eyes of individual participants. Participants with TFPD did not show a significant myopic shift (Fig 2). There was a significant difference in the slope of the linear fit between participants with LCHADD and participants with TFPD (linear regression slope for LCHAD, −0.24; slope for TFP, −0.036; difference, $P < 0.033$).

Electroretinography

Participants with LCHADD demonstrated diffusely attenuated electroretinography amplitudes with prolonged implicit times at an early age, whereas TFPD patients maintained normal electroretinography responses (Fig 3). Change over time was greater

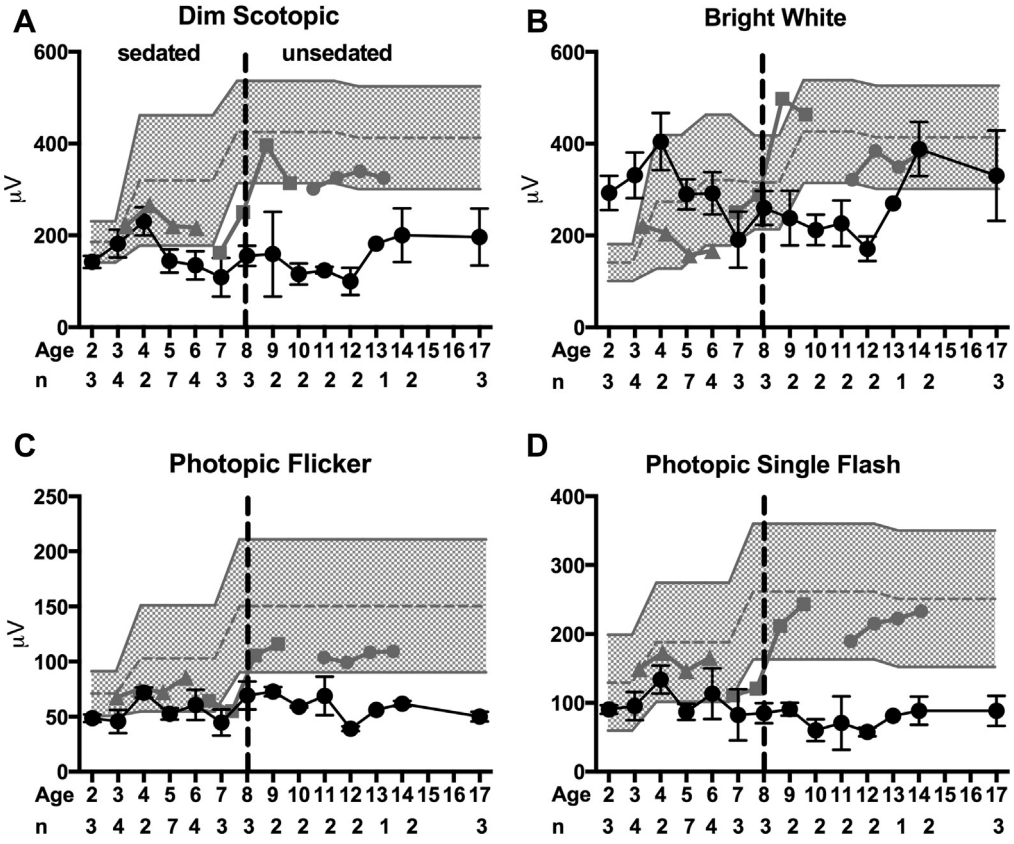

Figure 3. Electroretinograms showing the mean ± standard error of the mean of the (**A**) dim scotopic flash B-wave amplitude, (**B**) bright scotopic flash B-wave amplitude, (**C**) 30-Hz photopic flicker amplitude, and (**D**) photopic single flash B-wave amplitude in 2 groups of participants by age. The participants were divided into those with long-chain 3-hydroxyacyl-CoA dehydrogenase deficiency (LCHADD) (black circle; n for each age given below *x*-axis) and those with trifunctional protein deficiency (TFPD) (n = 1 participant at each age; grey triangle is patient LC18; gray square is patient LC17; grey circle is patient LC16). The normal range of values for each age is shown by gray shading. Participants were sedated for the test up to 8 years of age, and thereafter performed the test awake. The dashed line demarcates sedated and unsedated values. The presence of 1 allele of c.1528G→C was associated with lower dim and bright scotopic amplitudes as well as lower photopic and photopic single flash amplitudes.

among participants with LCHADD compared with participants with TFPD for all electroretinography parameters ($P < 0.05$ for group differences, repeated-measures analysis of variance). Long-chain 3-hydroxyacyl-CoA dehydrogenase deficiency was associated with lower scotopic and photopic B-wave amplitudes (Fig 3; for specific values, see Table S2, available at www.aaojournal.org), suggesting that both rods and cones are affected in this disease. These electroretinography changes were seen as early as 6 years of age, often followed by increased rate of decline (Fig 3).

Posterior Segment Findings

The fundus of participants with LCHADD exhibited a characteristic sequence of changes (Fig 4A). Early in the disease course, there is macular pigment clumping, followed by a progressive patchy chorioretinal atrophy that starts at the macula, with relative foveal sparing, and extends peripherally. Three participants with advanced disease demonstrated a hyperpigmented foveal scar (Table 2). Trifunctional protein deficiency patients maintained a normal funduscopic appearance (Fig 4B).

Posterior Segment Imaging

Fundus autofluorescence imaging in LCHADD patients demonstrated patchy areas of hypoautoflorescence with intervening bridges of intact autofluorescence, suggesting a sparse reticular network of relatively preserved RPE (Fig 5). On spectral-domain OCT imaging, early LCHADD disease showed irregularity of the interdigitation zone outside of the fovea (Fig 6). With time, there was patchy loss of ellipsoid zone and subjacent RPE. Regions of tissue loss have abrupt transition between healthy and diseased tissue. At this margin of atrophy, many eyes also have a notable scrolling of outer retinal elements and outer retinal tubulations (ORTs). Three eyes with advanced chorioretinopathy had subfoveal hyperreflective material consistent with scar formation. Optical coherence tomography images were not available in TFPD participants for comparison.

Two patients with LCHADD chorioretinopathy underwent OCT angiography (Fig 7). One patient is heterozygous for the LCHADD common mutation and is the oldest patient with the longest follow-up in our cohort. The other patient is homozygous for the common mutation and, although younger, has advanced disease. Optical coherence tomography angiography demonstrated marked loss of choriocapillaris that was far more extensive than

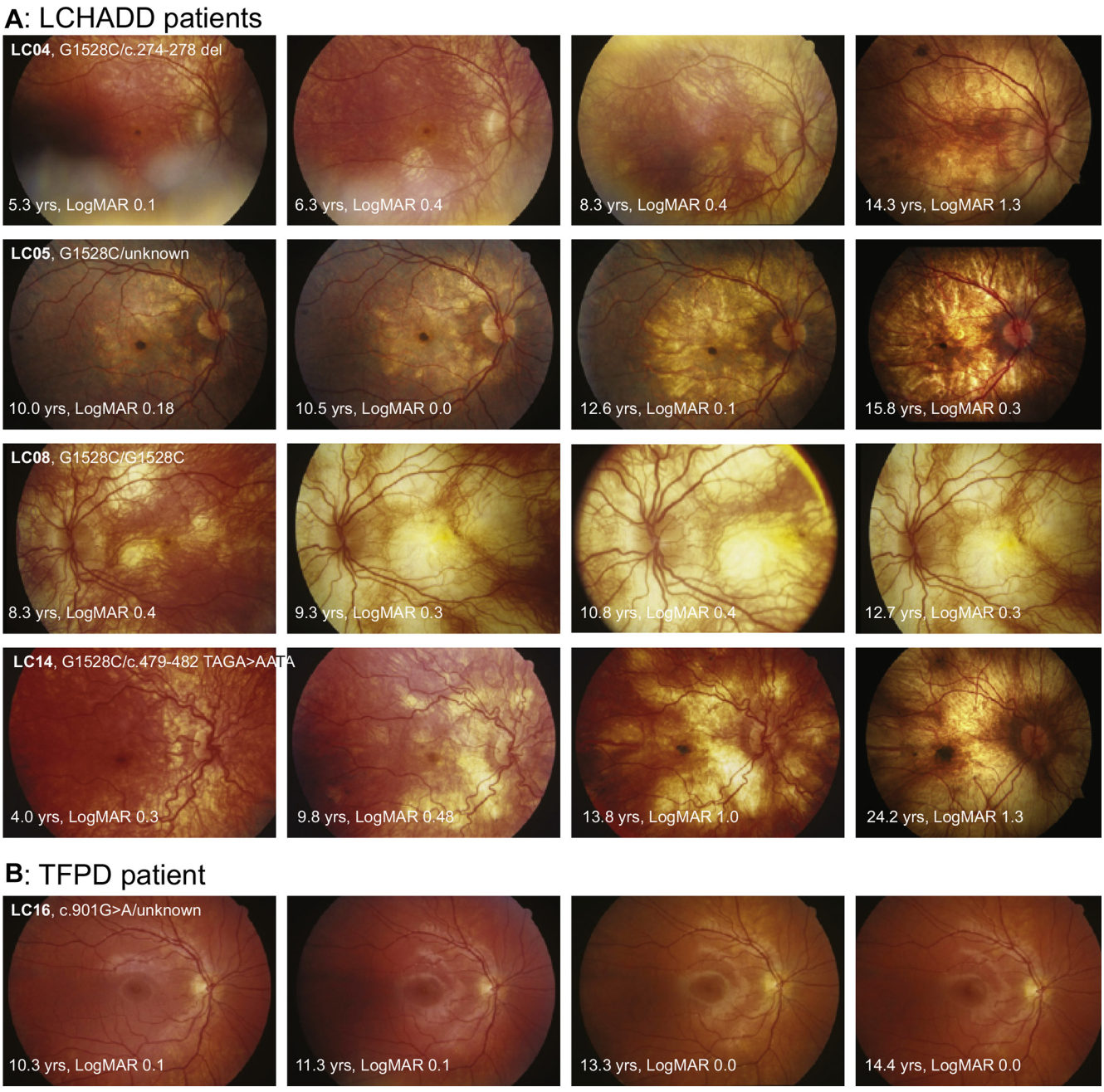

Figure 4. **A**, Disease progression despite dietary modification and systemic disease control in several patients with long-chain 3-hydroxyacyl-CoA dehydrogenase deficiency (LCHADD). Supratitles in each row indicate the patient and identified genetic mutations. Early in the disease, there is an accumulation of pigment at the central macula, which is followed by a progressive patchy chorioretinal atrophy of the posterior pole. With time, the atrophy extends to involve the periphery. In some participants, there is relative sparing of peripapillary retina. Late stages of the disease show the development of a subfoveal pigmentary scar (not in all patients). There is minimal retinal vascular attenuation or disc pallor. **B**, Color fundus photographs demonstrating disease stability in 1 patient with trifunctional protein deficiency (TFPD). Supratitles indicate the patient and identified genetic mutations. Unlike the LCHADD patients, participants with TFPD did not have any evidence of pigment clumping or chorioretinal atrophy. The fundus photographs of participant LC16 remained normal over 4.1 years of photographic follow-up. Although not included within the figure, the remaining 2 participants with TFPD also did not have any notable changes on fundus photography. logMAR = logarithm of the minimum angle of resolution.

photoreceptor loss as assessed by ellipsoid zone integrity (Fig 7). Coregistered FAF imaging demonstrated corresponding RPE loss, although due to low signal, it was difficult to compare the extent of RPE loss with choriocapillaris loss reliably. No TFPD participants underwent OCT angiography imaging.

Discussion

Long-chain 3-hydroxyacyl-CoA dehydrogenase deficiency, but not TFPD, continues to cause progressive chorioretinopathy and myopia, despite modern medical and dietary

Table 2. Chorioretinopathy Staging at First and Last Documented Examinations for Each Participant Demonstrating Progression of Disease with Time

Patient Identification	Age (yrs)	Visual Acuity (Logarithm of the Minimum Angle of Resolution)		Spherical Equivalent (D)		Chorioretinopathy Staging		Age (yrs)	Visual Acuity (Logarithm of the Minimum Angle of Resolution)		Spherical Equivalent (D)		Chorioretinopathy Staging	
		Right Eye	*Left Eye*	*Right Eye*	*Left Eye*	*Right Eye*	*Left Eye*		*Right Eye*	*Left Eye*	*Right Eye*	*Left Eye*	*Right Eye*	*Left Eye*
LCHADD														
LC01	6.7	0.54	0.3	−2.75	−2.38	2	2	12.5	0.3	0.3	−6.25	−4.50	3	3
LC02	3.2	CSM	CSM	−1.00	−1.00	2	2	6.8	0.8	1.0	−4.75	−4.88	4	4
LC03	0.8	CSM	CSM	+2.25	+2.25	1*	1*	5.8	0.5	0.3	+0.25	+0.63	2	2
LC04	5.3	0.1	0.1	−0.63	−0.63	2	2*	14.3	1.3	0.3	−5.50	−5.50	4*	4*
LC05	9.5	0.3	0.1	−1.63	−1.00	3	3	15.8	0.3	0.4	−9.50	−8.88	3*	3*
LC06	5.2	0.0	0.0	+1.00	+1.00	2	2	7.6	0.1	0.1	+0.63	+0.50	2/2	2
LC07	4.0	0.2	0.3	−1.50	−1.50	2	2	6.4	0.2	0.1	−2.00	−2.00	3/3	3
LC08	8.3	0.4	0.4	−0.50	−0.50	3	3	12.7	0.2	1.0	−8.00	−7.75	4/4	4
LC09	11.1	−0.1	−0.1	+1.12	+1.94	3	2	14.6	0.0	0.1	−1.88	−0.88	3/3	3
LC10	17.7	0.9	0.0	−5.13	−5.25	4+*	4+*	18.0	1.0	0.0	−5.13	−5.25	4+*	4+*
LC11	0.8	CSM	CSM	+1.50	+0.75	2*	2*	2.9	CSM	CSM	+1.25	+1.25	2/2	2
LC12	1.4	CSM	CSM	−0.50	−0.50	2*	2*	5.3	0.0	0.0	−0.75	−1.00	2/2	2
LC13	7.3	0.6	0.1	0.00	+1.13	2	2	9.8	1.0	0.7	−0.63	0.00	3*	3*
LC14	4.8	0.3	0.3	—	—	2	2	24.2	1.3	0.1	−3.75	−4.25	4+/4	4
LC15	0.4	CSM	CSM	−0.88	−0.88	—	—	11.3	0.3	0.4	—		—	—
LC25	11.8	0.2	1.5	−3.23	−4.13	4+*	4*	14.2	0.4	1.4	−3.25	−4.25	4+	4
LC27	1.6	CSM	CSM	—		—	—	9.2	−0.1	0.0	−0.38	−0.13	2*	2*
LC31	1.4	CSM	CSM	+2.50	+2.50	1*	1*	5.4	0.0	0.0	+0.88	+1.00	1*	1*
TFPD														
LC16	10.3	0.1	0.1	+0.93	+1.07	1	1	14.4	0.0	−0.1	0.00	0.00	2/2	2
LC17	4.7	0.0	0.0	+0.63	+0.68	1	1	8.7	0.0	0.0	+0.38	+0.38	1/1	1
LC18	1.0	CSM	CSM	+0.75	+1.00	2	2	3.0	CSM	CSM	+0.25	+0.25	2/2	2

CSM = central, steady, and maintained; D = diopters; LCHADD = long-chain 3-hydroxyacyl-CoA dehydrogenase deficiency; TFPD = trifunctional protein deficiency; — = unavailable data.
Examination descriptions and fundus photographs were used to stage the chorioretinopathy using the fundus staging criteria developed by Tyni et al.[12] The stage "4+" is not included within the staging criteria of Tyni et al, but included to designate times when foveal scarring was appreciated on examination. Corresponding ages, visual acuity (logarithm of the minimum angle of resolution), and spherical equivalent were included for visits if available. Participant LC15 did not have fundus photographs or examination descriptions available to stage.
*No fundus photograph was available; in these cases, grading was based solely on clinical data.

interventions to manage systemic comorbidity. The chorioretinopathy begins with changes that are mostly within the macula and posterior pole and creates paracentral scotomas on static and kinetic testing that enlarge, deepen, and coalesce with time. As demonstrated on the static visual fields, the pathologic features are weighted toward the center portion of the field, but do not have the consistent radial or bilateral symmetry seen in most forms of retinitis pigmentosa.[22] Although the variability may be influenced by diet, some of the variability may relate to stochastic events. Our findings on in vivo spectral-domain OCT and OCT angiography analysis, derived from the largest series on MTP disorder-associated chorioretinopathy with some of the oldest known participants, suggested once again that photoreceptor degeneration may be secondary to an insult in either the RPE or choriocapillaris. These tissue layers may be optimal targets for future treatment approaches.

Structural assessment with en face multimethod imaging including OCT angiography demonstrated that RPE and choriocapillaris loss was more extensive than photoreceptor loss (Fig 7) in participants with LCHADD. Furthermore, the outer retina was noted to scroll at the margins of degeneration with formation of ORTs (Fig 6). Outer retinal tubulations have been noted in a number of degenerative conditions of the RPE and choriocapillaris, including geographic atrophy and choroideremia.[23,24] A prevailing theory is that photoreceptors form ORTs as a survival strategy in the context of loss of trophic support from a degenerating RPE or choriocapillaris.[25]

In general, visual field loss in LCHADD correlates well with the anatomic changes seen in the disease. In studying the relationship between outer retina structure and field changes in retinitis pigmentosa, Smith et al[26] found that the absence of the ellipsoid zone correlated well with loss of sensitivity greater than 7.6 dB from normal. A similar structure−function correlation was found in LCHADD patient LC14: the left eye at 24.2 years of age had preservation of a region of field where the sensitivity defect was less than 7.6 dB. Furthermore, in that same eye, ORTs were present in the retina just temporal to the fovea (Fig 6C), which corresponded to the region of retained sensitivity just nasal to fixation in the static visual field (Fig S2, available at www.aaojournal.org). This finding is consistent with the theory of ORT formation

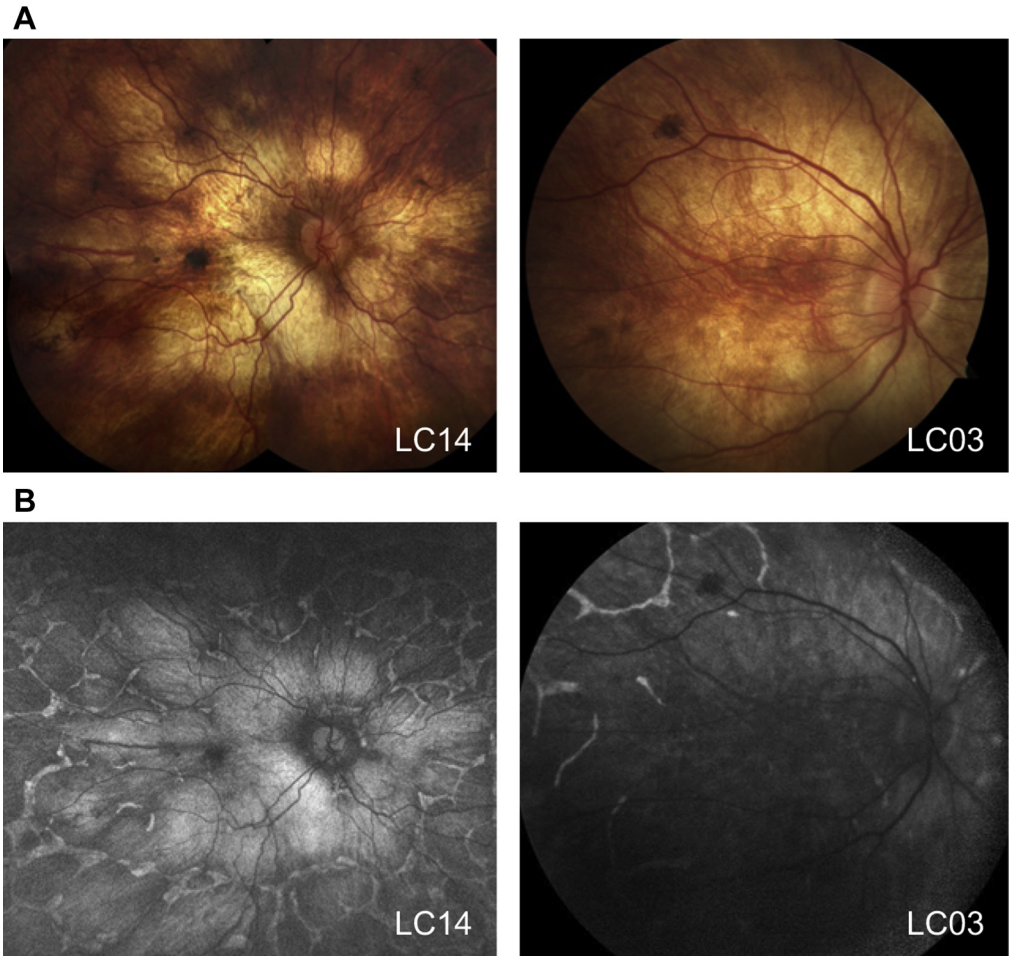

Figure 5. Widefield autofluorescence imaging demonstrating extensive retinal pigment epithelium (RPE) loss that is worst in the posterior pole corresponding to areas of atrophy. **A**, Montage of color fundus photographs demonstrating patchy RPE atrophy extending beyond the mid periphery of 2 patients (patients LC03 and LC14) with advanced long-chain 3-hydroxyacyl-CoA dehydrogenase deficiency. **B**, Corresponding wide-field fundus autofluorescence images from the same patients from the same year (patient LC03) and 3 years later (patient LC14) demonstrating extensive RPE loss in the posterior pole. There is a network of residual RPE hyperautofluorescence around well-demarcated nummular regions of RPE loss in the periphery. The diffusely bright signal in areas of RPE loss is thought to be most consistent with scleral autofluorescence, but may represent artifact from wavelength overlap between exciting and detected light.

being an adaptive mechanism that helps to preserve retinal function.

Our findings of early RPE degeneration provide in vivo corroboration of prior findings from histopathologic and cell culture studies. Two postmortem specimens from eyes with LCHADD chorioretinopathy demonstrated macrophage infiltration of the RPE.[8] More recently, a study of patient-specific induced pluripotent stem cell-derived RPE cells containing the LCHAD mutation demonstrated that these cells were smaller, were more irregularly shaped, and were held together by disorganized tight junctions as compared with normal RPE cells in culture. The affected cells had fewer melanosomes, an increased number of melanolysosomes, and a pathologic accumulation of lipid.[27] In addition to substantiating these findings, our in vivo assessment with OCT angiography allows for longitudinal evaluation of eyes with better preservation of tissue architecture.

Wide-field FAF imaging has proven to be a valuable clinical tool to characterize the extent of degeneration in affected eyes. These images highlight the initial posterior involvement with relative foveal sparing (Fig 5). Subsequent degeneration in the midperiphery, with large scalloped regions of atrophy with an intervening network of relatively preserved RPE, is somewhat reminiscent of other chorioretinopathies such as gyrate atrophy and choroideremia.

Interestingly, despite the early degeneration in the posterior pole, participants tended to retain good central acuity in at least 1 eye. Participants with profound central vision loss frequently exhibited elevated pigmented subfoveal scars. Without histopathologic correlation, the exact nature of this hyperpigmented scar remains uncertain. Optical coherence tomography imaging in 1 participant demonstrated a subfoveal scar adjacent to a large break in Bruch's membrane suggestive of a prior choroidal neovascularization membrane (CNVM). Alternatively, this

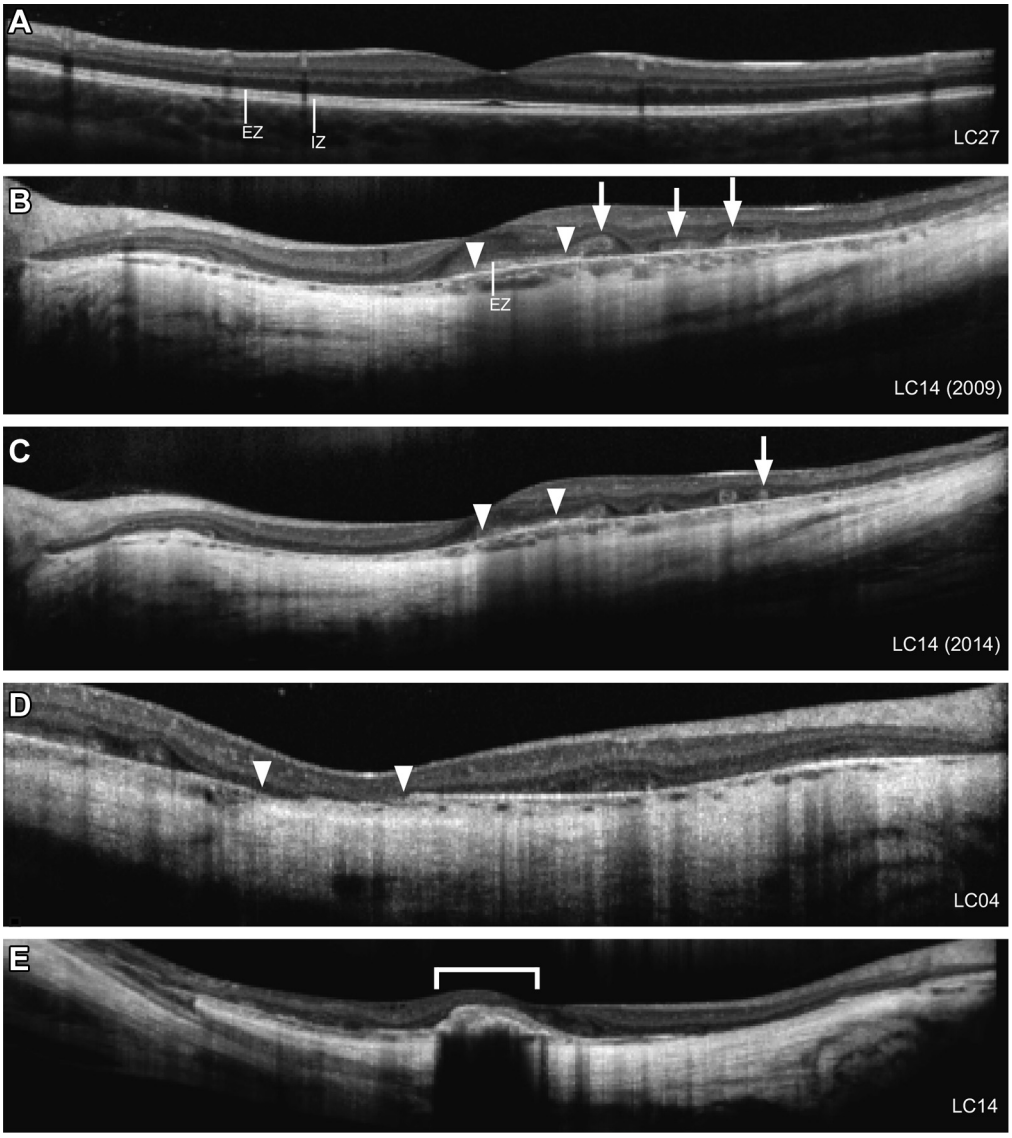

Figure 6. Optical coherence tomography images demonstrating progressive atrophy in long-chain 3-hydroxyacyl-CoA dehydrogenase deficiency with abrupt transition zones and outer retinal tubulations. **A**, Early disease shows mild irregularity of the interdigitation zone (IZ). **B**, Ellipsoid zone (EZ) and retinal pigment epithelium (RPE) loss in later stages is characterized by abrupt transition zones (inverted triangles) with scrolling of outer retinal elements and outer retinal tubulations at the margins of degeneration (arrows). **C**, Same eye as in (**B**) 5 years later demonstrating progressive outer retinal atrophy approaching the fovea (inverted triangles) and additional outer retinal tubulation formation (arrows). Some eyes have (**D**) apparent breaks in Bruch's membrane (inverted triangles) and (**E**) subfoveal hyperpigmented scars (bracket) suggestive of a prior choroidal neovascular membrane. Nearly all patients had foveal EZ sparing in at least 1 eye.

pigmented lesion may result from accumulation of inwardly migrating, diseased RPE cells from surrounding tissue or an idiopathic gliosis. Two prior reports describe the development of a similar subfoveal scar,[28,29] one with an active CNVM.[20] Although we did not detect any active CNVM, the finding of a subfoveal scar in 17% of our patients calls for close monitoring of central acuity in affected eyes, perhaps with Amsler grid testing. Acutely symptomatic patients should be evaluated promptly for consideration of anti−vascular endothelial growth factor treatment. Previously, posterior staphyloma has been suggested as the cause of vision loss in patients with LCHADD.[11] Because of the rarity of the disease, a meta-analysis of visual function and chorioretinopathy among long-term survivors would be helpful to better elucidate the frequency of these findings and the cause of visual dysfunction.

The lengthy follow-up in this study highlights that progressive myopia in LCHADD continues into adulthood. It is unclear if high axial myopia may represent a comorbid condition with associated degenerative changes, perhaps contributing to CNVM formation. No participants demonstrated peripheral retinal pathologic features such as lattice degeneration or retinal tears.

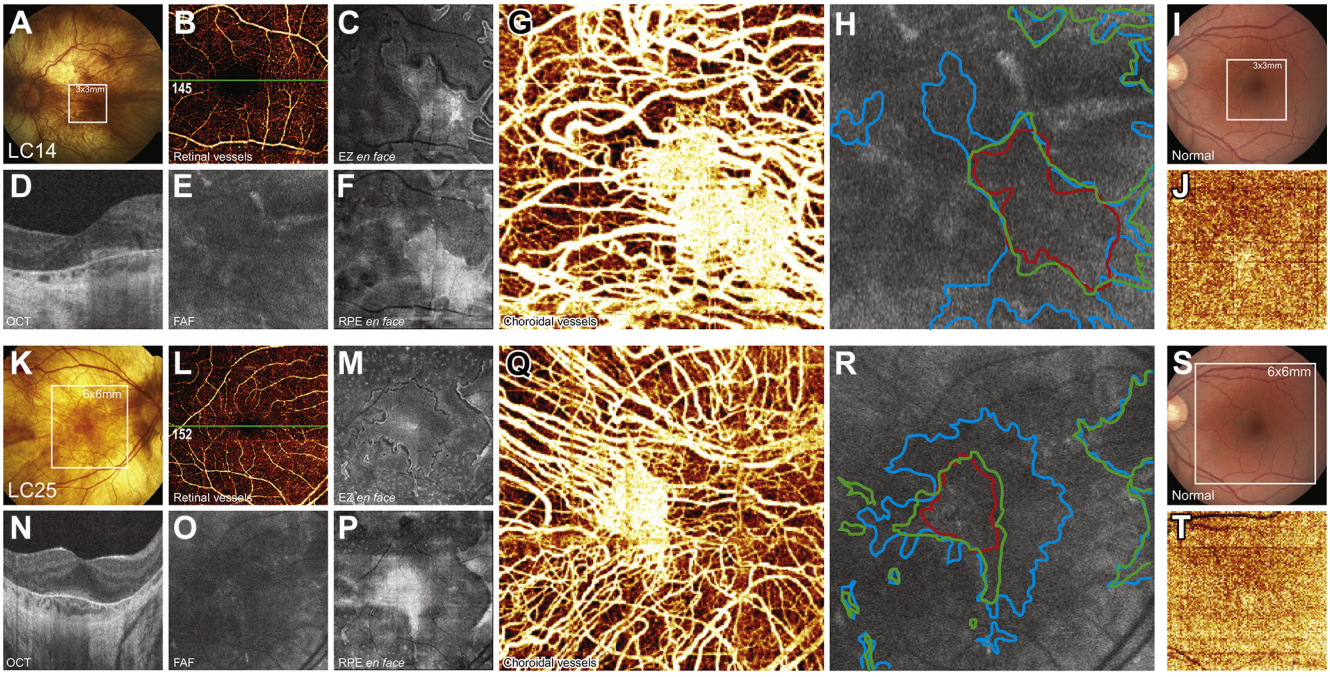

Figure 7. En face imaging with optical coherence tomography (OCT) angiography suggesting that the retinal pigment epithelium (RPE) and choriocapillaris loss precede ellipsoid zone (EZ) loss in long-chain 3-hydroxyacyl-CoA dehydrogenase deficiency (LCHADD): (**A**–**H**) patient LC14, (**I**, **J**) 3×3-mm control participant, (**K**–**R**) patient LC25, and (**S**, **T**) 6×6-mm control participant. **A**, **K**, Color fundus photographs outlining the 3×3-mm and 6×6-mm locations of the OCT angiography scans, respectively. **D**, **N**, Optical coherence tomography cross-section through the fovea as shown on retinal vessel OCT angiogram (**B**, **L**). **E**, **O**, Corresponding 3×3-mm and 6×6-mm fundus autofluorescence (FAF) images, respectively. **C**, **M**, En face OCT slab of the EZ within the outer retina. **F**, **P**, En face OCT slab of the RPE. **G**, **Q**, Choroidal OCT angiogram demonstrating a small area of preserved choriocapillaris; surrounding choriocapillaris atrophy results in direct visualization of underlying larger choroidal vessels. **H**, **R**, Overlay of EZ (blue; from [**C**] and [**M**]), choriocapillaris (red; from [**G**] and [**Q**]), and RPE (green; from [**F**] and [**P**]) margins on autofluorescence image. **J**, **T**, Choroidal OCT angiography images from a control retina for 3×3-mm and 6×6-mm scanning areas, corresponding to **I** and **S**, respectively. Density of healthy choriocapillaris in (**J**) and (**T**) masks underlying larger choroidal vessels.

Despite affecting the same enzyme complex, LCHADD and TFPD are 2 distinct clinical entities with highly disparate ophthalmic findings. Patients with LCHADD have a greater accumulation of potentially toxic metabolites produced by selective loss of LCHAD function with relative preservation of the long-chain hydratase activity compared with relatively low concentrations of metabolites among patients with TFPD and loss of all 3 enzymatic functions.[30] The theory that toxic metabolites are part of the underlying cause of chorioretinopathy in LCHADD is supported by studies linking low serum 3-hydroxyacylcarnitines and fatty acid byproducts to a milder ophthalmic phenotype, even among patients with the same genotype.[6] A competing theory suggests that the mutated subunit of LCHADD induces retinal cell death by a dominant negative mechanism, possibly through interference of nearby enzymes.[10,30,31] Further research is needed to determine the cause of these disparate ophthalmic phenotypes among patients with mutations in the same enzyme complex.

This study has limitations. Because of the retrospective study design in this exceedingly rare condition, follow-up is variable with an evolving imaging workup over the course of the study. For instance, evaluation with the novel OCT angiography technology was performed on only 2 participants. Second, in several patients, the modern molecular testing techniques failed to identify 2 deleterious mutations, possibly because of pathogenic intronic or splice-site variants. However, the diagnosis was established in each participant through robust clinical assessment and enzymatic assays of cultured skin fibroblasts. Finally, dietary intake and metabolic control was assessed at a moment in time, but both factors are dynamic, changing from day to day and from moment to moment. There was no way to determine all of the metabolic decompensation episodes in our patients followed up in multiple clinics around the United States.

To our knowledge, this is the largest series demonstrating the ophthalmic manifestations of MTP disorders, and this series has the longest follow-up. With some of the oldest living patients with these diseases, our study provides greater understanding of the clinical progression of these metabolic diseases in the era of improved dietary and metabolic control. Advanced imaging techniques have provided some of the first in vivo evidence suggesting that photoreceptor damage may be secondary to atrophy of the RPE, choriocapillaris, or both. This finding suggests that the RPE or choriocapillaris may be optimal target tissues for prospective treatments, such as gene therapy. Our series also helps to provide prognostic information to

patients; we showed that patients with TFPD have minimal clinical and functional retinal changes, whereas LCHADD patients often progress despite continued medical and dietary treatment.

References

1. Wanders RJ, IJlst L, van Gennip AH, et al. Long-chain 3-hydroxyacyl-CoA dehydrogenase deficiency: identification of a new inborn error of mitochondrial fatty acid beta-oxidation. J Inherit Metab Dis 1990;13:311–4.
2. Rinaldo P, Matern D, Bennett MJ. Fatty acid oxidation disorders. Annu Rev Physiol 2002;64:477–502.
3. Tyni T, Pihko H. Long-chain 3-hydroxyacyl-CoA dehydrogenase deficiency. Acta Paediatr 1999;88:237–45.
4. Przyrembel H, Jakobs C, IJlst L, et al. Long-chain 3-hydroxyacyl-CoA dehydrogenase deficiency. J Inherit Metab Dis 1991;14:674–80.
5. Boer den ME, Wanders RJ, Morris AA, et al. Long-chain 3-hydroxyacyl-CoA dehydrogenase deficiency: clinical presentation and follow-up of 50 patients. Pediatrics 2002;109:99–104.
6. Gillingham MB, Weleber RG, Neuringer M, et al. Effect of optimal dietary therapy upon visual function in children with long-chain 3-hydroxyacyl CoA dehydrogenase and trifunctional protein deficiency. Mol Genet Metab 2005;86:124–33.
7. Gillingham M. Optimal dietary therapy of long-chain 3-hydroxyacyl-CoA dehydrogenase deficiency. Mol Genet Metab 2003;79:114–23.
8. Tyni T, Pihko H, Kivelä T. Ophthalmic pathology in long-chain 3-hydroxyacyl-CoA dehydrogenase deficiency caused by the G1528C mutation. Curr Eye Res 1998;17:551–9.
9. Bertini E, Dionisi-Vici C, Garavaglia B, et al. Peripheral sensory-motor polyneuropathy, pigmentary retinopathy, and fatal cardiomyopathy in long-chain 3-hydroxy-acyl-CoA dehydrogenase deficiency. Eur J Pediatr 1992;151:121–6.
10. Fletcher AL, Pennesi ME, Harding CO, et al. Observations regarding retinopathy in mitochondrial trifunctional protein deficiencies. Mol Genet Metab 2012;106:18–24.
11. Tyni T, Kivelä T, Lappi M, et al. Ophthalmologic findings in long-chain 3-hydroxyacyl-CoA dehydrogenase deficiency caused by the G1528C mutation. Ophthalmology 1998;105:810–24.
12. Tyni T, Immonen T, Lindahl P, et al. Refined staging for chorioretinopathy in long-chain 3-hydroxyacyl coenzyme A dehydrogenase deficiency. Ophthal Res 2012;48:75–81.
13. Pons R, Roig M, Riudor E, et al. The clinical spectrum of long-chain 3-hydroxyacyl-CoA dehydrogenase deficiency. Pediatr Neurol 1996;14:236–43.
14. Smith EH, Matern D. Acylcarnitine Analysis by Tandem Mass Spectrometry. Hoboken, NJ: John Wiley & Sons, Inc.; 2001. 17.8.1−17.8.20.
15. Weleber RG, Smith TB, Peters D, et al. VFMA: topographic analysis of sensitivity data from full-field static perimetry. Transl Vis Sci Technol 2015;4:14:1−13.
16. Schiefer U, Pascual JP, Edmunds B, et al. Comparison of the new perimetric GATE strategy with conventional full-threshold and SITA standard strategies. Invest Ophthalmol Vis Sci 2009;50:488–94.
17. Luithardt AF, Meisner C, Monhart M, et al. Validation of a new static perimetric thresholding strategy (GATE). Br J Ophthalmol 2015;99:11–5.
18. Jia Y, Tan O, Tokayer J, et al. Split-spectrum amplitude-decorrelation angiography with optical coherence tomography. Optics Express 2012;20:4710–25.
19. Gao SS, Liu G, Huang D, Jia Y. Optimization of the split-spectrum amplitude-decorrelation angiography algorithm on a spectral optical coherence tomography system. Opt Lett 2015;40:2305–8.
20. McCulloch DL, Marmor MF, Brigell MG, et al. ISCEV Standard for full-field clinical electroretinography (2015 update). Doc Ophthalmol 2015;130:1–12.
21. Holladay JT. Visual acuity measurements. J Cataract Refract Surg 2004;30:287–90.
22. Massof RW, Finkelstein D, Starr SJ, et al. Bilateral symmetry of vision disorders in typical retinitis pigmentosa. Br J Ophthalmol 1979;63:90–6.
23. Goldberg NR, Greenberg JP, Laud K, et al. Outer retinal tubulation in degenerative retinal disorders. Retina 2013;33:1871–6.
24. Jain N, Jia Y, Gao SS, et al. Optical coherence tomography angiography in choroideremia: correlating choriocapillaris loss with overlying degeneration. JAMA Ophthalmol 2016;134:697–702.
25. Ma N, Streilein JW. Contribution of microglia as passenger leukocytes to the fate of intraocular neuronal retinal grafts. Invest Ophthalmol Vis Sci 1998;39:2384–93.
26. Smith TB, Parker M, Steinkamp PN, et al. Structure-Function modeling of optical coherence tomography and standard automated perimetry in the retina of patients with autosomal dominant retinitis pigmentosa. PLoS One 2016;11:e0148022.
27. Polinati PP, Ilmarinen T, Trokovic R, et al. Patient-specific induced pluripotent stem cell-derived RPE cells: understanding the pathogenesis of retinopathy in long-chain 3-hydroxyacyl-CoA dehydrogenase deficiency. Invest Ophthalmol Vis Sci 2015;56:3371–82.
28. Fahnehjelm KT, Holmström G, Ying L, et al. Ocular characteristics in 10 children with long-chain 3-hydroxyacyl-CoA dehydrogenase deficiency: a cross-sectional study with long-term follow-up. Acta Ophthalmol 2007;86:329–37.
29. Stopek D, Gitteau Lala E, Labarthe F, et al. Long-chain 3-hydroxyacyl CoA dehydrogenase deficiency and choroidal neovascularization [in French]. J Fr Ophtalmol 2008;31:993–8.
30. Spiekerkoetter U, Khuchua Z, Yue Z, et al. General mitochondrial trifunctional protein (TFP) deficiency as a result of either alpha- or beta-subunit mutations exhibits similar phenotypes because mutations in either subunit alter TFP complex expression and subunit turnover. Pediatr Res 2004;55:190–6.
31. Wang Y, Mohsen AW, Mihalik SJ, et al. Evidence for physical association of mitochondrial fatty acid oxidation and oxidative phosphorylation complexes. J Biol Chem 2010;285:29834–41.

Footnotes and Financial Disclosures

Originally received: February 20, 2016.
Final revision: June 11, 2016.
Accepted: June 16, 2016.
Available online: ■■■. Manuscript no. 2016-353.

[1] Casey Eye Institute, Oregon Health & Science University, Portland, Oregon.

[2] Department of Ophthalmology, Emory University, Atlanta, Georgia.

[3] Molecular & Medical Genetics, Oregon Health & Science University, Portland, Oregon.

Financial Disclosure(s):
The author(s) have made the following disclosure(s): Y.J.: Patent — Optovue, Inc., Fremont, California.

C.O.H.: Consultant — BioMarin Pharmaceutical, San Fafael, California; Financial support (to institution) — BioMarin Pharmaceutical, San Rafael, California; Cydan, Inc., Cambridge, Massachusetts; National PKU Alliance, Tomahawk, Wisconsin; Lecturer — BioMarin Pharmaceutical, San Rafael, California

D.H.: Financial support, Equity owner — Optovue, Inc., Fremont, California; Patent — Optovue, Inc., Fremont, California; Carl Zeiss Meditec, Inc., Dublin, California.

R.G.W.: Consultant — Novartis, Cambridge, Massachusetts; Pfizer, New York, New York; Wellstat, Gaithersburg, Maryland; Advisory board — AGTC, Alachua, Florida; Foundation Fighting Blindness, Columbia, Maryland; Financial support - Sanofi, Bridgewater, New Jersey; Patent — VFMA 8,657,446; Dr. Weleber serves on advisory boards for the Foundation Fighting Blindness (this relationship has been reviewed and managed by OHSU).

M.E.P.: Consultant — AGTC, Alachua, Florida; IONIS Pharmaceuticals, Carlsbad, California; Spark Therapeutics, Philadelphia, Pennsylvania; Editas, Cambridge, Massachusetts; Financial support — AGTC, Alachua, Florida; Sanofi, Bridgewater, New Jersey

Supported by Research to Prevent Blindness, Inc., New York, New York (unrestricted departmental funding); Foundation Fighting Blindness, Columbia, Maryland (ECDA to M.E.P.; CDA CF-CL-0614-0647-OHSU [NJ]; CDA C-CL-0711-0534-OHSU01 [R.G.W.]); the National Eye Institute, National Institutes of Health, Bethesda, Maryland (grant nos.: P30 EY010572, R01 EY023285 [D.H.], R01 EY024544 [Y.J.], and DP3 DK104397 [Y.J.]); Clinical and Translational Science Award, Bethesda, Maryland (grant no.: UL1TR000128 [Y.J., D.H.]); the Food and Drug Administration, Silver Spring, Maryland (M.B.G.); the American Diabetes Association, Alexandria, Virginia (M.B.G.); and the Choroideremia Research Foundation, Springfield, Massachusetts (M.E.P.). The sponsors or funding organizations had no role in the design or conduct of this research.

Author Contributions:

Conception and design: Boese, Jain, Jia, Schlechter, Harding, Gao, Patel, Huang, Weleber, Gillingham, Pennesi

Analysis and interpretation: Boese, Jain, Jia, Harding, Gao, Patel, Huang, Weleber, Gillingham, Pennesi

Data collection: Boese, Jain, Jia, Schlechter, Harding, Gao, Patel, Huang, Weleber, Gillingham, Pennesi

Obtained funding: none

Overall responsibility: Boese, Jain, Jia, Schlechter, Harding, Gao, Patel, Huang, Weleber, Gillingham, Pennesi

Abbreviations and Acronyms:
BCVA = best-corrected visual acuity; **BM** = Bruch's membrane; **CNVM** = choroidal neovascularization membrane; **ffERG** = full-field electroretinogram; **FAF** = fundus autofluorescence; **logMAR** = logarithm of the minimum angle of resolution; **LCHADD** = long-chain 3-hydroxyacyl-CoA dehydrogenase deficiency; **MTP** = mitochondrial trifunctional protein; **OCT** = optical coherence tomography; **OHSU** = Oregon Health & Science University; **ORT** = outer retinal tubulation; **RPE** = retinal pigment epithelium; **TFP** = trifunctional protein; **TFPD** = trifunctional protein deficiency.

Correspondence:
Mark E. Pennesi, MD, PhD, Ophthalmic Genetics, Casey Eye Institute—Marquam Hill, 3375 SW Terwilliger Boulevard, Portland, OR 97239-4197. E-mail: pennesim@ohsu.edu.